Global evaluation of biofuel potential from microalgae

Jeffrey W. Moody[a], Christopher M. McGinty[b], and Jason C. Quinn[a,1]

[a]Mechanical and Aerospace Engineering and [b]Department of Wildland Resources, Utah State University, Logan, UT 84322

Edited by Stephen Polasky, University of Minnesota, St. Paul, MN, and approved April 29, 2014 (received for review November 18, 2013)

In the current literature, the life cycle, technoeconomic, and resource assessments of microalgae-based biofuel production systems have relied on growth models extrapolated from laboratory-scale data, leading to a large uncertainty in results. This type of simplistic growth modeling overestimates productivity potential and fails to incorporate biological effects, geographical location, or cultivation architecture. This study uses a large-scale, validated, outdoor photobioreactor microalgae growth model based on 21 reactor- and species-specific inputs to model the growth of *Nannochloropsis*. This model accurately accounts for biological effects such as nutrient uptake, respiration, and temperature and uses hourly historical meteorological data to determine the current global productivity potential. Global maps of the current near-term microalgae lipid and biomass productivity were generated based on the results of annual simulations at 4,388 global locations. Maximum annual average lipid yields between 24 and 27 $m^3 \cdot ha^{-1} \cdot y^{-1}$, corresponding to biomass yields of 13 to 15 $g \cdot m^{-2} \cdot d^{-1}$, are possible in Australia, Brazil, Colombia, Egypt, Ethiopia, India, Kenya, and Saudi Arabia. The microalgae lipid productivity results of this study were integrated with geography-specific fuel consumption and land availability data to perform a scalability assessment. Results highlight the promising potential of microalgae-based biofuels compared with traditional terrestrial feedstocks. When water, nutrients, and CO_2 are not limiting, many regions can potentially meet significant fractions of their transportation fuel requirements through microalgae production, without land resource restriction. Discussion focuses on sensitivity of monthly variability in lipid production compared with annual average yields, effects of temperature on productivity, and a comparison of results with previous published modeling assumptions.

algae | global model | geographic information system | life cycle assessment | dynamic map

Recent volatility in oil prices, attributed to increased demand and limited resources, has led to the development of unconventional petroleum reserves, such as oil sands, and increased exploration of alternative and renewable fuel sources. Scalability limitations associated with traditional terrestrial biofuel feedstocks have renewed interest in next-generation feedstocks, such as microalgae. Microalgae offer many potential advantages over traditional terrestrial oil crops, including higher lipid productivities, a lack of competition for arable land, year-round cultivation, integration with saline and low-quality water sources, and a viable drop-in equivalent fuel product (1–5). These scalable advantages make microalgae a promising feedstock for biofuel production and a potential sustainable alternative to traditional petroleum fuels.

The current near-term productivity potential for microalgae at large-scale currently is being estimated through the linear scaling of laboratory-based growth and lipid data, which has led to a large variance in reported values (4, 6). This type of scaling has been integrated into various life cycle, technoeconomic, and resource models of the microalgae-to-biofuels process, leading to unrealistic assumptions about industrial function, and is a source of large uncertainty (2). Current near-term algal lipid productivity values reported in life cycle, technoeconomic, and resource modeling literature range from 2.3 $m^3 \cdot ha^{-1} \cdot y^{-1}$ reported by Ramachandra et al. (6) to 136.9 $m^3 \cdot ha^{-1} \cdot y^{-1}$ reported by Mata et al. (4), with a variety of researchers reporting values between these two extremes (1, 3–26). Large uncertainty in the reported productivity potentials stems from the use of simplistic growth modeling through simple solar conversion calculations or linear scaling of laboratory data; both fail to incorporate biological function and geographic diversity. Propagation of errors in microalgae production modeling at large-scale skew life cycle, economic, and scalability assessments, because lipid yield typically represents the functional unit in these assessments.

Decreasing uncertainty in the current productivity potential from microalgae requires increased fidelity in growth modeling through temporal and biological resolution combined with geographically specific climatic and resource data (27). This study integrates a microalgae growth model with hourly historical meteorological data from various global locations for the assessment of the current near-term lipid and biomass productivity potential of microalgae cultivated in a traditional closed-system photobioreactor. The microalgae growth and lipid content is simulated on an hourly time scale over the course of 1 y at 4,388 global locations through the use of 12–25 y (depending on site) of meteorological data. Results from annual simulations were surface interpolated to produce a dynamic global map of the current near-term microalgae lipid productivity and are intended to represent the current large-scale production potential based on a photobioreactor architecture. Discussion focuses on the effects of temperature on productivity, a geographically specific scalability assessment, monthly variability in productivity, and a comparison of modeled results with current near-term productivity potentials reported in microalgae biofuel life cycle, technoeconomic, and scalability literature.

Results and Discussion

The results from this study are divided into four sections: (*i*) baseline global lipid productivity and variability, (*ii*) temperature sensitivity to lipid productivity, (*iii*) global scalability, and (*iv*) comparison of results with literature-based modeling assumptions.

Significance

Research into microalgae as a feedstock for biofuels continues to increase because of the inherent potential advantages it holds over traditional terrestrial feedstocks. However, the true near-term large-scale productivity of microalgae remains uncertain. This study integrates a large-scale, outdoor growth model with historical meteorological data from 4,388 global locations to estimate the current near-term lipid and biomass productivity potential from microalgae cultivated in a photobioreactor architecture. Results show that previous life cycle, technoeconomic, and resource assessments dramatically overestimated lipid yields. A scalability assessment that leverages geographic information systems data to evaluate the current productivity potential from microalgae with global fuel consumption and land availability shows that microalgae can have a positive impact on the transportation energy portfolios of various countries.

Author contributions: J.C.Q. designed research; J.W.M., C.M.M., and J.C.Q. performed research; and J.W.M., C.M.M., and J.C.Q. wrote the paper.

The authors declare no conflict of interest.

This article is a PNAS Direct Submission.

Freely available online through the PNAS open access option.

[1]To whom correspondence should be addressed. E-mail: jason.quinn@usu.edu.

This article contains supporting information online at www.pnas.org/lookup/suppl/doi:10.1073/pnas.1321652111/-/DCSupplemental.

Global Productivity Potential and Variability. Hourly biomass and lipid productivity results from simulation locations were averaged for an annual geographically resolved result. Results from the 4,388 simulation locations were surface interpolated to produce a dynamic map illustrating the current near-term lipid productivity potential from microalgae across the globe (Fig. 1). The closed photobioreactor system modeled represents a promising production system compared with that of an open raceway pond, based on increased stability and improved volumetric productivity from extended surface area and a short light path. Results from this closed system will be greater than those of an open system (1, 22, 28). As expected, locations in the northern and southern parts of the globe, where the light intensity and temperature are lower, result in decreased lipid productivity compared with regions more centrally located. Although locations around the equator typically are considered optimum cultivation locations because of their annual temperature stability, results show these locations do not necessarily produce the largest lipid yields; this is the result of other climatic phenomena that affect biological growth. A detailed comparison of four countries, India, China, Brazil, and Australia, is presented in Fig. 2. Manaus, Brazil, is closer to the equator than Alice Springs, Australia, but experiences more rain and cloud cover, and as a result, Manaus produces a lower lipid and biomass yield, 18.9 $m^3 \cdot ha^{-1} \cdot y^{-1}$ and 10.2 $g \cdot m^{-2} \cdot d^{-1}$, respectively, compared with the lipid and biomass yield in Alice Springs, 24.2 $m^3 \cdot ha^{-1} \cdot y^{-1}$ and 13.1 $g \cdot m^{-2} \cdot d^{-1}$, respectively. India and China are neighboring countries, but India has better average lipid yields, primarily because of temperature differences. In general, the temperature in India is closer than that of China to the optimal growth temperature and demonstrates the growth model's ability to accurately capture temperature effects.

Results also illustrate a nonlinear relationship between biomass growth and lipid productivity. A biomass yield of 6,720 $kg \cdot ha^{-1} \cdot y^{-1}$ is found in both Ostrov Vrangelja, Russia, and Lomnicky Stit, Slovakia, with corresponding lipid productivities of 3.37 $m^3 \cdot ha^{-1} \cdot y^{-1}$ and 3.26 $m^3 \cdot ha^{-1} \cdot y^{-1}$, respectively. The 3.3% difference in lipid production is not intended to be statistically significant but is used to illustrate the biological model's ability to capture nontrivial biological effects, including nitrogen quota, inoculation lipid content, light availability, and temperature. The lipid percentage of the biomass is not fixed and varies based on biological factors. A dynamic global map of the current predicted biomass productivity is presented in *SI Appendix*.

Highest and lowest monthly yields from 11 locations across the globe are presented in Table 1. The variability changes from location to location, primarily because of climatic diversity. Locations with low variability and large annual lipid yields represent areas where cultivation typically does not shut down because of cold conditions and operates year round. For example, Learmonth, Australia, has a higher average monthly lipid yield but a large variability compared with Cali, Columbia. The economic impacts associated with variability suggest that Cali, Columbia, would be a superior location even though it has a slightly lower monthly average lipid productivity compared with Learmonth, Australia (14); this is because higher variability requires increased infrastructure, which negatively affects biorefinery economics. Global variability maps are presented in *SI Appendix*.

Locations found in the northern and southern hemispheres, such as Poltavka, Bagaskar, Punta Arenas, and Rio Gallegos, demonstrate a large variability and low average monthly lipid yields because of large swings in climate as a result of geographic location, with colder climates resulting in a winter shut-down. Alternatively, Yuma, Arizona, United States, is a desert location that does not shut down in the winter but reaches temperatures that far exceed the optimum temperature in the summer, resulting in a lower lipid yield. Kisumu, Kenya, whose average annual temperature is closer to optimum conditions, achieves a higher lipid yield. These examples illustrate that deviation from optimum temperature in either direction has a negative impact on the biomass and lipid productivity of the system.

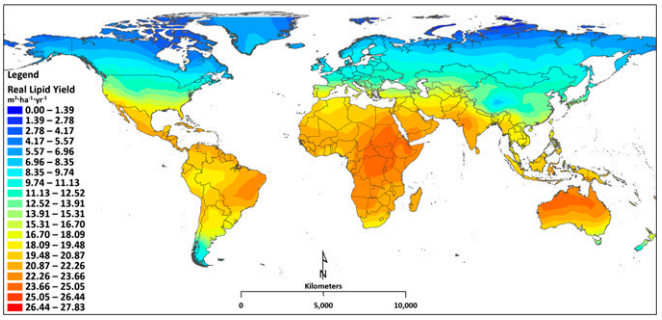

Fig. 1. World map of the current near-term lipid productivity potential from microalgae based on a validated biological growth model representative of *Nannochloropsis* cultivated in a photobioreactor. Results are based on the simulation of 4,388 geographical locations.

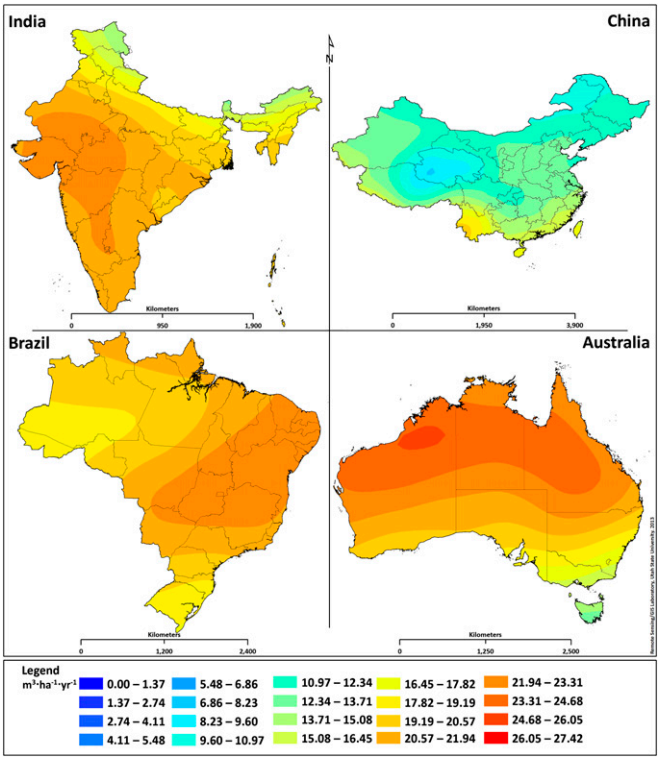

Fig. 2. Current lipid productivity maps for India, China, Brazil, and Australia.

Temperature Sensitivity. A temperature sensitivity analysis demonstrates the importance of considering the effect of temperature on productivity. Pilot plant facilities currently are using waste heat or raw energy to maintain culture temperature in cold months to sustain production (9). Large-scale implementation of this technique is limited as the result of resource availability and the economics associated with raw energy. Waste heat and raw energy for maintaining temperature will be limited to inoculum and small-scale pilot plant facilities.

Results for simulations in which ideal temperature is maintained are presented in Fig. 3. Compared with the nonideal temperature results presented in the baseline scenario (Fig. 1), the current lipid productivity across the globe is dramatically higher for the ideal scenario, illustrating the nontrivial effect that maintaining optimum temperature has on microalgae growth and lipid productivity. The locations situated in the most

Table 1. Average microalgae lipid yields in cubic meters per hectare^{-1} per meter^{-1} (corresponding biomass yields in grams per meter^{-2} per day^{-1}) of various regions around the world with respective high and low monthly lipid yields

Location	Lipid and biomass yield		
	Maximum monthly	Average monthly	Lowest monthly
Kisumu, Kenya	2.47 (15.9)	2.28 (14.8)	2.07 (13.3)
Learmonth, Australia	2.61 (18.0)	2.16 (14.0)	1.49 (9.64)
Trivandrum, India	2.42 (15.6)	2.08 (13.4)	1.75 (11.3)
Cali, Columbia	2.27 (14.6)	2.04 (13.2)	1.91 (12.3)
Hawaii, United States	2.36 (15.3)	1.97 (12.8)	1.50 (9.95)
Yuma, AZ, United States	2.68 (17.3)	1.80 (11.7)	0.68 (5.16)
Poltavka, Russia	2.30 (14.8)	1.06 (6.84)	0.46 (3.23)
Bagaskar, Finland	2.19 (14.1)	0.77 (5.00)	0.55 (3.86)
Punta Arenas, Chile	1.77 (11.9)	0.77 (5.07)	0.51 (3.25)

northern and southern parts of the globe are affected dramatically when comparing ideal temperature results with real temperature lipid productivity. Bryce Canyon, Utah, for example, has an ideal and nonideal lipid yield of 22 $m^3 \cdot ha^{-1} \cdot y^{-1}$ (biomass yield of 11.9 $g \cdot m^{-2} \cdot d^{-1}$) and 10.7 $m^3 \cdot ha^{-1} \cdot y^{-1}$ (biomass yield of 5.8 $g \cdot m^{-2} \cdot d^{-1}$), corresponding to a 106% increase for maintaining optimum temperature. The dramatic increase predominantly is a result of extending the growing season from 214 d to 365 d. The 365 d/y assumes no facility shutdown and no culture crashes, which may be expected in the system modeled (9). Integrating waste heat from industrial processing plants makes it feasible for locations to achieve improved lipid productivity, but heat resource availability ultimately will limit the scalability.

Scalability Assessment. A scalability assessment was performed to determine the feasibility of a microalgae growth, lipid extraction, and conversion-based microalgae-to-biofuels process to meet various energy demands of global nations. The current near-term lipid productivity results from this study are combined with land availability data for a geographic realized assessment. Water, nitrogen and phosphorous nutrients, and CO_2 were assumed to be readily available. The oil consumption for various regions (29) was combined with nonarable land statistics based on the Global Land Cover 2000 (GLC2000) dataset (30) and the productivity results from this study. Results were used to evaluate the hypothetical potential impact that microalgal-derived biofuels might make with respect to a given region's oil consumption. ArcGIS was used to reduce the land cover from the GLC2000 database to obtain nonarable and agricultural land statistics for each country around the world (30). The scalability assessment, which focuses on biodiesel production, includes a 90% efficiency for the extraction of lipids from the biomass, a 90% efficiency for the conversion of oil to fuel, and a 0.8 packing factor, which accounts for facility infrastructure (25) to more accurately represent the microalgae-to-biofuel process at industrial scale. The assessment demonstrates the hypothetical potential microalgae has for supplementing energy and reducing demand for traditional fossil oil, as well as the lipid yield advantage microalgae hold over traditional terrestrial crops, such as soybeans (Table 2).

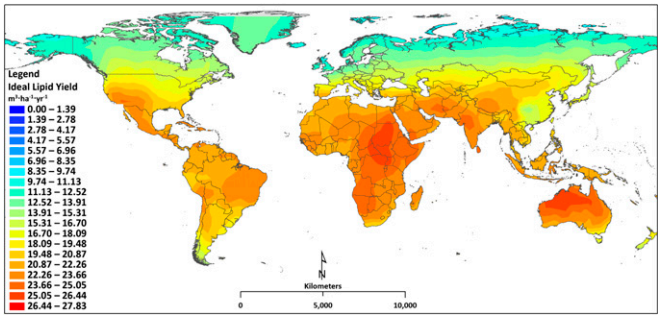

Fig. 3. Map of the current lipid productivity for maintaining optimum temperature throughout the year.

Results from Table 2 show it is feasible for Brazil, Canada, the United States, and China to replace 30% of their petroleum oil consumption based on utilization of poor-quality land for microalgae cultivation and processing. Japan, however, requires over 100% of its nonarable land to replace 30% of its transportation fuel consumption through microalgae. However, these results are based on current modeled productivity values and do not extrapolate for future improvement potential. A table representing the amount of agricultural land needed to supplement 30% of oil consumption for other countries around the world, based on the lipid yield of microalgae from this study compared with soybeans, is presented in *SI Appendix*. Further investigation of actual land suitable for microalgae cultivation, such as slope restriction, is needed to provide a more accurate assessment. Inclusion of resource restrictions, such as water, nutrients, and CO_2, will decrease microalgae potential further.

Literature Comparison. The large variation in current microalgae productivity in the literature makes it difficult to perform accurate life cycle, technoeconomic, and resource assessments, as productivity represents the functional unit of these studies and dramatically affects results. The life cycle, technoeconomic, and resource assessments in the literature use a wide range of productivity assumptions that are higher and lower than the productivities presented in this study, resulting in a large spread of end results regardless of processing pathway differences.

Modeling assumptions in terms of lipid yield for various life cycle, technoeconomic, and resource assessments are compared with the results of this study. Various growth systems are modeled in the different assessments, including open raceway ponds and photobioreactors. The results from this study represent a promising production scenario based on cultivation in closed photobioreactors, which have been demonstrated to be robust culture platforms (1, 9, 22, 28). To make a direct comparison of values presented in the literature with results from this study, conversions of literature data were performed and are detailed in *SI Appendix*. The map of the current near-term lipid productivity potential (Fig. 1) was rescaled to encompass the range of lipid productivity results found in the literature (Fig. 4). Locations with the highest lipid productivities in this study fall in the lower third of literature assumptions. These results show that most of the productivity potentials reported in the literature and integrated into the life cycle, technoeconomic, and resource assessments of microalgae-based biofuels make optimistic assumptions in terms of the current near-term productivity potential. Results from the optimistic lipid productivity assumptions favorably skew the economic and environmental impact of microalgae-based biofuels.

Table 2. Amount of nonarable land needed to supplement 30% of oil consumption for different regions around the world based on replacement by microalgae

Location	Nonarable land, ha	30% of transportation fuel consumption, $L{\cdot}y^{-1}$	Microalgae biodiesel production potential, $L{\cdot}y^{-1}$	Nonarable land required, %
Brazil	2.06E+07	4.38E+10	2.79E+11	16
Canada	3.63E+08	3.63E+10	1.65E+12	2
China	2.22E+08	1.90E+11	1.79E+12	11
Japan	9.16E+04	7.62E+10	7.49E+08	10,000
United States	7.03E+07	2.86E+11	5.80E+11	49

The validated model in this study demonstrates that lipid productivity is a dynamic variable that cannot be assumed to be constant temporally or geographically. Future assessments of the microalgae-to-biofuels production process require site-specific assessments that incorporate geographically realized biological growth modeling to improve the validity and accuracy of results and must incorporate the availability of water, nutrients (such as nitrogen and phosphorus), and CO_2. Including these resource limitations will further reduce the level of biofuel production potential.

Methods

The following sections present details on the thermal and biological growth models representative of *Nannochloropsis* cultivated in a photobioreactor architecture. Thermal and biological modeling was performed in MATLAB, with results processed and land availability statistics generated using Esri ArcGIS (31).

Photobioreactor Thermal and Biological Growth Models. The modeled photobioreactor system is submerged in a shallow pool of water, which serves as the structural and passive thermal support of the system. The photobioreactor system consists of equally spaced reactors, 0.05 m thick, 0.3 m tall, and 17.4 m long, constructed of 0.12-mm polyethylene (detailed pictures and schematics are presented in *SI Appendix*). The biological growth model, representative of *Nannochloropsis*, requires 21 inputs, with light and temperature serving as the primary inputs (2). A thermal model of the shallow pool is used to represent the temperature of the system accurately. The temperature of the shallow pool (assumed to be equivalent to the photobioreactor temperature, with calculations presented in *SI Appendix*) and corresponding meteorological conditions serve as the primary inputs to the growth model that predicts biomass and lipid content. Validation of the model was performed through the collection of 9 wk of biological growth and meteorological data at the Solix test bed facility in Fort Collins, Colorado. All model assumptions, validation, and details for the thermal and biological growth models are presented in Quinn et al. (27).

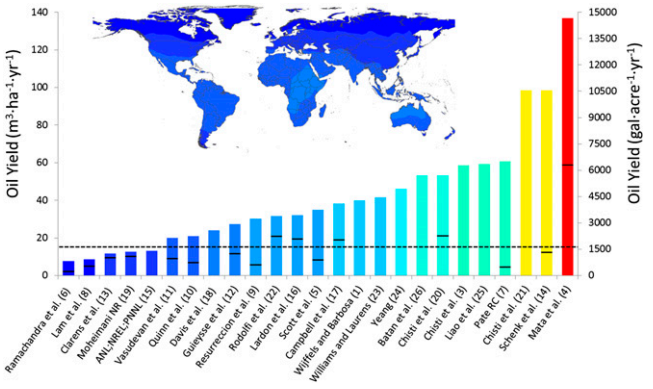

Fig. 4. Oil yield assumptions found in life cycle, technoeconomic, and scalability assessments compared with the results of this study presented as a global map, Fig. 1 rescaled to capture the range of literature values. Because of the range of productivities reported in some studies, the low end of the range is represented by the black line and the color bar represents the high end reported. The black dashed line represents the world average current near-term lipid productivity of 17 $m^3{\cdot}ha^{-1}{\cdot}y^{-1}$ corresponding to a biomass yield of 9.4 $g{\cdot}m^{-2}{\cdot}d^{-1}$ as determined in this study.

The time-resolved biological growth model incorporates 21 reactor- and species-specific inputs to accurately model the biomass and lipid productivity of *Nannochloropsis* based on real-world climatic and thermal conditions (27). *Nannochloropsis* is a promising strain for biofuel production because of its characteristically high lipid content (9, 21, 32). The model captures growth through carbon uptake, assuming a 50% carbon content (2, 33), and includes photosynthetic rate (P_c), respiration rate (rR_c), and biosynthetic energy required for nitrogen uptake (Ψ) to calculate the growth rate (μ):

$$\mu = P_c - rR_c - \Psi. \quad [1]$$

The temperature dependency of photosynthesis is modeled through the corresponding effect on ribulose-biphosphate carboxylase (RuBisCO) activity and is an efficiency factor that affects P_c. The enzyme activity as a function of temperature is modeled based on a bell-shaped curve, with the optimal temperature at the peak corresponding to the maximum temperature efficiency (φ_T) (34). Deviating from the ideal temperature in either direction corresponds to a decrease in temperature efficiency, with the temperature efficiency factor being a dimensionless number between 0 and 1, as presented in Eq. **2**:

$$\varphi_T = \frac{2 \cdot e^{\left(\frac{Ea}{R \cdot T_{opt}} \frac{Ea}{R \cdot T}\right)}}{1 + e^{\left(\frac{Ea}{R \cdot T_{opt}} \frac{Ea}{R \cdot T}\right)^2}}. \quad [2]$$

From Eq. **2**, the optimum temperature (23 °C for the modeled species) is captured in T_{opt}, R is the ideal gas constant, Ea is the activation energy of carboxylation RuBisCO, and T is the culture temperature calculated in the thermal model. The thermal model of the growth system accounts for heat loss and gain from conduction, convection, evaporation, and solar incidence (a detailed picture is presented in *SI Appendix*). The model incorporates the climatic variables of atmospheric pressure, cloud cover, wind speed, wind direction, dry-bulb temperature, dew-point temperature, and solar radiation to predict the temperature of the shallow basin. The thermal model is used to calculate the culture temperature and input to the biological growth model. The effect of the temperature efficiency factor on growth is illustrated in *SI Appendix*. For global modeling, the temperature efficiency is dynamic and calculated on an hourly basis at each simulation location. Cultivation is assumed to shut down and stays dormant when the basin temperature falls below freezing, with cultivation resuming upon thaw.

A lipid model was created and incorporated into the biological growth model to accurately predict the microalgae lipid production based on nitrogen, temperature, and light intensity effects. This model is based on a nitrogen trigger, with cell function switching from protein to lipid synthesis while maintaining a mass balance among the lipid, carbohydrate, and protein:

$$m_B = m_L + m_C + m_P, \quad [3]$$

where m_B is the mass of the biomass and m_L, m_C, and m_P are the mass of the lipid, carbohydrate, and protein, respectively.

Weather Data. Historical hourly meteorological weather data serve as a primary input to the thermal and biological growth model. EnergyPlus Weather (EPW) data files from the Department of Energy and the American Society of Heating, Refrigeration and Air Conditioning Engineers were obtained for 4,388 global locations (35, 36). It is important to note that the weather data in some countries may be less accurate depending on the way the data were collected. The EPW data files are derived from hourly weather data originally archived at the US National Climatic Data Center. The databases contain weather observations of wind speed and direction, sky cover, visibility, ceiling height, dry-bulb temperature, dew-point temperature, atmospheric pressure, and liquid precipitation for 12–25 y, depending on location.

Observed data were processed statistically to generate standard 1-y datasets representative of historically observed weather data or EPW data files (36). Hourly solar radiation is calculated through a model based on the sun–earth geometry, observed cloud cover, relative humidity, and wind speed (36). Total solar radiation is converted to photosynthetically active radiation for biological modeling (37). The climatic variables from the EPW data files are used as the primary inputs to the thermal and biological growth models.

Simulation Architecture. ***Harvest technique and reporting metrics.*** The biological growth model was operated with a time-based harvest schedule. Cultures were inoculated at a density of 1 $g{\cdot}L^{-1}$ at hour zero and harvested after 160 h or a biomass density of 3 $g{\cdot}L^{-1}$, whichever occurred first. Each harvest retains biomass that is used as inoculum for the next growth cycle. This harvest technique is representative of the operation of the research and development and pilot plant facility used for model validation (9). The current near-term productivity potentials reported are based on a photosynthetic area of the thermal pond basin where the photobioreactor system resides and do not include the infrastructure required for large-scale cultivation. Additionally, the reported potentials represent the biological lipid production and do not include losses associated with lipid extraction and conversion to fuel. The scalability assessment extends the analysis to include a lipid extraction and conversion process. The assessment assumes a packing factor of 0.8 (25) to account for facility infrastructure and a 90% efficiency for extraction and a 90% efficiency for the conversion of oil to fuel (38) to represent the microalgae to biofuel process more accurately. Water, nutrients (such as nitrogen and phosphorus), and CO_2 availability were not considered limiting in the scalability assessment.

Temperature sensitivity. The effects of temperature on the current near-term potential lipid productivity were examined further as part of this study. Typical laboratory-based studies regulate temperature to optimum conditions to maximize production or remove it as a variable (32, 39). However, temperature control at large-scale represents an economically unfavorable option based on the amount of raw energy required. Some pilot plant facilities are using waste heat from colocated industrial processing facilities or raw energy to maintain optimum temperatures, but resource limits the scalability (9, 40). A second set of simulations was performed in which the temperature efficiency in the biological growth model was fixed to optimum conditions $(\varphi_T = 1)$. The corresponding biomass and lipid productivities are compared with the nonideal case. Realistically, temperature will not be controlled at large-scale based on resource and economic limitations. Large-scale systems can use waste heat to support inoculation systems; thus, the results from the optimum scenario may be applied in select modeling applications or pilot-plant siting.

Productivity variability. Results from a harmonization effort among the Argonne National Laboratory, National Renewable Energy Laboratory, and Pacific Northwest National Laboratory (14) show that an increase in economic costs, as well as global warming potential, is associated with microalgae biofuel systems with high production variability. Previous assessments focused on reporting the current annual average lipid productivity potential and failed to investigate and report the minimum and maximum lipid productivities throughout the year (27, 41). Most modeling efforts do not have the fidelity to investigate variability, because a fixed growth rate and lipid percentage typically are assumed. Productivity in a biological system depends on resource availability, specifically sunlight. Global positioning over the course of a year will cause variability in this resource, affecting growth. This study presents a variability assessment for each simulated location, with results for the highest and lowest monthly lipid productivities based on a temporal resolution of 1 mo. Months with the highest lipid yield were compared with the average annual monthly yield and lowest monthly yield. The lowest monthly yield was found by considering only months that produced one full harvest coming out of a water basin thaw.

Geographical Information System. The results from the 4,388 simulations were interpolated over the globe using a surface interpolation. Surface interpolation is a methodology used to develop values for unmeasured locations by using measured or simulated values from known neighboring locations (31). Many interpolation algorithms have been developed to account for spatial and statistical differences of data; however, the central principal of surface interpolation algorithms is the application of the weighted sum of data values from nearby locations to produce an estimated value for any given location within the maximum spatial constraints of the data. Interpolation algorithms have been used to calculate surface values that depict current and historic climate values (42, 43), to extract and estimate land surface features (44), and to evaluate the impacts of noise from aircraft and industry on the surrounding environment (45).

This research used the surface interpolation tools available in the Esri ArcGIS 10.2 Geostatistical Analyst extension. ArcGIS also was used to reduce the land cover from the GLC2000 database to obtain the nonarable land statistics for each country around the world (30). The ordinary kriging method was used to explore the data values for lipids and biomass because of the spatial point sample data of this analysis (*SI Appendix*, Fig. S5). Ordinary kriging does not assume the mean of the data is constant over the entire spatial domain, rather that the mean is constant in local spatial neighborhoods (31). This helps compensate further for the impacts of clustered groups by assigning points within a clustered group less overall weight than isolated data points. This is an important consideration in this analysis, because data points tend to be highly clustered in more densely populated regions and lipid and biomass production tend to be higher in areas nearer the equator and to decrease toward the polar regions. It should be noted that there are some cases in which the general trend is affected by elevation and climate; however, the consistency of the data allows for the use of ordinary kriging methods.

Model validation outputs, including predicted error, standardized error, and normal QQ plots, were evaluated for each surface interpolation model to verify suitable performance. Manual accuracy testing also was conducted by withholding a random selection of 25% of the global data points, performing an interpolation analysis, and then sampling and regressing the observed data against the predicted interpolated surface values. The R^2 between the interpolated and observed data was 0.97, further sustaining the conclusion that the surface interpolation methods were performed adequately.

Conclusion

Alternatives to fossil fuels, such as microalgae-based biofuels, are being investigated because of their promising productivity potential along with other sustainable advantages compared with traditional terrestrial feedstocks. However, a large uncertainty exists with regard to the current lipid productivity potential from microalgae. This study uses a validated outdoor photobioreactor biological growth model to determine the current near-term lipid productivity potential of microalgae around the world by integrating hourly meteorological data at 4,388 sites. Results are spatially interpolated to generate a global map. The effect of temperature and variability on microalgae growth shows that temperature plays a critical role in yield, and variability must be considered in large-scale assessments. The lipid productivity results from this study fall into the lower third of the life cycle, technoeconomic, and resource assessments currently found in the literature, with the highest global lipid yields based on results from this study ranging between 24 and 27 $m^3{\cdot}ha^{-1}{\cdot}y^{-1}$ (corresponding biomass yields of 13–15 $g{\cdot}m^{-2}{\cdot}d^{-1}$). The results from this work show that even with an optimistic photobioreactor production system, most of the modeling work being used in assessments overestimates productivity. A scalability analysis incorporating geographical information system land classification statistics and results from this study show that many regions can supplement 30% of their fuel consumption through microalgae by using nonarable land. Future life cycle, technoeconomic, and scalability assessments will require integration of geographically and temporally resolved biological growth modeling for increased fidelity.

ACKNOWLEDGMENTS. We gratefully acknowledge financial support from Department of Energy Grant DE-EE0003114.

1. Wijffels RH, Barbosa MJ (2010) An outlook on microalgal biofuels. *Science* 329(5993): 796–799.
2. Quinn J, de Winter L, Bradley T (2011) Microalgae bulk growth model with application to industrial scale systems. *Bioresour Technol* 102(8):5083–5092.
3. Chisti Y (2007) Biodiesel from microalgae. *Biotechnol Adv* 25(3):294–306.
4. Mata TM, Martins AA, Caetano NS (2010) Microalgae for biodiesel production and other applications: A review. *Renew Sustain Energy Rev* 14(1):217–232.
5. Scott SA, et al. (2010) Biodiesel from algae: Challenges and prospects. *Curr Opin Biotechnol* 21(3):277–286.
6. Ramachandra TV, Madhab MD, Shilpi S, Joshi NV (2013) Algal biofuel from urban wastewater in India: Scope and challenges. *Renew Sustain Energy Rev* 21: 767–777.
7. Lam MK, Lee KT (2012) Microalgae biofuels: A critical review of issues, problems and the way forward. *Biotechnol Adv* 30(3):673–690.

8. Resurreccion EP, Colosi LM, White MA, Clarens AF (2012) Comparison of algae cultivation methods for bioenergy production using a combined life cycle assessment and life cycle costing approach. *Bioresour Technol* 126:298–306.
9. Quinn JC, et al. (2012) *Nannochloropsis* production metrics in a scalable outdoor photobioreactor for commercial applications. *Bioresour Technol* 117:164–171.
10. Vasudevan V, et al. (2012) Environmental performance of algal biofuel technology options. *Environ Sci Technol* 46(4):2451–2459.
11. Guieysse B, Béchet Q, Shilton A (2013) Variability and uncertainty in water demand and water footprint assessments of fresh algae cultivation based on case studies from five climatic regions. *Bioresour Technol* 128:317–323.
12. Clarens AF, Resurreccion EP, White MA, Colosi LM (2010) Environmental life cycle comparison of algae to other bioenergy feedstocks. *Environ Sci Technol* 44(5): 1813–1819.
13. Schenk PM, et al. (2008) Second generation biofuels: High-efficiency microalgae for biodiesel production. *BioEnergy Res* 1(1):20–43.
14. Davis R, et al.; Argonne National Laboratory; National Renewable Energy Laboratory; Pacific Northwest National Laboratory (2012) *Renewable Diesel from Algal Lipids: An Integrated Baseline for Cost, Emissions, and Resource Potential from a Harmonized Model*. ANL/ESD/12-4; NREL/TP-5100-55431; PNNL-21437 (Argonne National Laboratory, Argonne, IL; National Renewable Energy Laboratory, Golden, CO; Pacific Northwest National Laboratory, Richland, WA).
15. Lardon L, Hélias A, Sialve B, Steyer JP, Bernard O (2009) Life-cycle assessment of biodiesel production from microalgae. *Environ Sci Technol* 43(17):6475–6481.
16. Campbell PK, Beer T, Batten D (2011) Life cycle assessment of biodiesel production from microalgae in ponds. *Bioresour Technol* 102(1):50–56.
17. Davis R, Aden A, Pienkos PT (2011) Techno-economic analysis of autotrophic microalgae for fuel production. *Appl Energy* 88(10):3524–3531.
18. Moheimani NR (2013) Long-term outdoor growth and lipid productivity of *Tetraselmis suecica*, *Dunaliella tertiolecta* and *Chlorella sp* (Chlorophyta) in bag photobioreactors. *J Appl Phycol* 25(1):167–176.
19. Chisti Y (2008) Response to Reijnders: Do biofuels from microalgae beat biofuels from terrestrial plants? *Trends Biotechnol* 26(7):351–352.
20. Chisti Y (2008) Biodiesel from microalgae beats bioethanol. *Trends Biotechnol* 26(3): 126–131.
21. Rodolfi L, et al. (2009) Microalgae for oil: Strain selection, induction of lipid synthesis and outdoor mass cultivation in a low-cost photobioreactor. *Biotechnol Bioeng* 102(1):100–112.
22. Williams PJL, Laurens LML (2010) Microalgae as biodiesel and biomass feedstocks: Review and analysis of the biochemistry, energetics and economics. *Energy Environ Sci* 3(5):554–590.
23. Yeang K (2008) Biofuel from algae. *Archit Des* 78(3):118–119.
24. Liao YF, Huang ZH, Ma XQ (2012) Energy analysis and environmental impacts of microalgal biodiesel in China. *Energy Policy* 45:142–151.
25. Batan L, Quinn J, Willson B, Bradley T (2010) Net energy and greenhouse gas emission evaluation of biodiesel derived from microalgae. *Environ Sci Technol* 44(20):7975–7980.
26. Pate RC (2013) Resource requirements for the large-scale production of algal biofuels. *Biofuels* 4(4):409–435.
27. Quinn JC, Catton K, Wagner N, Bradley TH (2012) Current large-scale US biofuel potential from microalgae cultivated in photobioreactors. *BioEnergy Res* 5(1):49–60.
28. Singh R, Sharma S (2012) Development of suitable photobioreactor for algae production–a review. *Renew Sustain Energy Rev* 16(4):2347–2353.
29. British Petroleum (2013) *BP Statistical Review of World Energy June 2013*. Available at http://bp.com/content/dam/bp/pdf/statistical-review/statistical_review_of_world_energy_2013.pdf. Accessed July 2013.
30. Bartholome E, Belward AS (2005) GLC2000: A new approach to global land cover mapping from Earth observation data. *Int J Remote Sens* 26(9):1959–1977.
31. Esri (2013) *ArcGIS 10.2 for Server Functionality Matrix*. Available at http://esri.com/library/brochures/pdfs/arcgis-server-functionality-matrix.pdf. Accessed October 2013.
32. Van Wagenen J, et al. (2012) Effects of light and temperature on fatty acid production in *Nannochloropsis salina*. *Energies* 5(3):731–740.
33. Anderson LA (1995) On the hydrogen and oxygen-content of marine phytoplankton. *Deep Sea Res Part I Oceanogr Res Pap* 42(9):1675–1680.
34. Alexandrov GA, Yamagata Y (2007) A peaked function for modeling temperature dependence of plant productivity. *Ecol Modell* 200(1-2):189–192.
35. US Department of Energy (2013) *Energy Efficiency and Renewable Energy*. Available at http://apps1.eere.energy.gov/buildings/energyplus/weatherdata_about.cfm?CFID=1458062&CFTOKEN=b5a223c3dab07751-BEBA1819-C408-0494-52E5262691596C2A&jsessionid=BBA0639311027A6BC68F8171BC89B680.eere. Accessed November 2012.
36. ASHRAE (2013) *ASHRAE International Weather Files for Energy Calculations 2.0 (IWEC2)*. Available at https://ashrae.org/resources–publications/bookstore/iwec2. Accessed March 2013.
37. Alados-Arboledas L, Olmo FJ, Alados I, Perez M (2000) Parametric models to estimate photosynthetically active radiation in Spain. *Agric Meteorol* 101(2-3):187–201.
38. Frank E, Han J, Palou-Rivera I, Elgowainy A, Wang M (2011) *Life-Cycle Analysis of Algal Lipid Fuels with the GREET Model* (Argonne National Laboratory, Argonne, IL).
39. Quinn JC, Turner CW, Bradley TH (2012) Scale-up of flat plate photobioreactors considering diffuse and direct light characteristics. *Biotechnol Bioeng* 109(2):363–370.
40. Sheehan J, Dunahay T, Benemann J, Roessler P (1998) *A Look Back at the US Department of Energy's Aquatic Species Program: Biodiesel from Algae* (National Renewable Energy Laboratory, Golden, CO).
41. Wigmosta MS, Coleman AM, Skaggs RJ, Huesemann MH, Lane LJ (2011) National microalgae biofuel production potential and resource demand. *Water Resour Res* 47(3):W00H04.
42. Daly C, et al. (2008) Physiographically sensitive mapping of climatological temperature and precipitation across the conterminous United States. *Int J Climatol* 28(15): 2031–2064.
43. Hijmans RJ, Cameron SE, Parra JL, Jones PG, Jarvis A (2005) Very high resolution interpolated climate surfaces for global land areas. *Int J Climatol* 25(15):1965–1978.
44. O'Callaghan JF, Mark DM (1984) The extraction of drainage networks from digital elevation data. *Comput Vis Graph Image Process* 28(3):323–344.
45. Ramsey R, McGinty C, Lowry J, Leydsman E (2012) *Grand Teton National Park and John D. Rockefeller, Jr. Memorial Parkway: Natural Resource Condition Assessment* (National Park Service, Fort Collins, CO).